IceBridge MCoRDS L1B Geolocated Radar Echo Strength Profiles, Version 2

USER GUIDE

How to Cite These Data

As a condition of using these data, you must include a citation:

Paden, J., J. Li, C. Leuschen, F. Rodriguez-Morales, and R. Hale. 2014, updated 2019. *IceBridge MCoRDS L1B Geolocated Radar Echo Strength Profiles, Version 2*. [Indicate subset used]. Boulder, Colorado USA. NASA National Snow and Ice Data Center Distributed Active Archive Center. https://doi.org/10.5067/90S1XZRBAX5N. [Date Accessed].

FOR QUESTIONS ABOUT THESE DATA, CONTACT NSIDC@NSIDC.ORG

FOR CURRENT INFORMATION, VISIT https://nsidc.org/data/IRMCR1B

National Snow and Ice Data Center

TABLE OF CONTENTS

1 DATA DESCRIPTION

1.1 Parameters

This Multichannel Coherent Radar Depth Sounder (MCoRDS) data set contains measurements for echograms, time, latitude, longitude, and elevation, as well as flight path charts and echogram images. The parameters are described in Table 1.

Table 1. File Parameter Description

Parameter	Description	Units
`Bottom`	Two-way travel time to bottom used during processing. Not the final picked bottom.	seconds
`Surface`	Estimated two-way propagation time to the surface from the collection platform. This uses the same frame of reference as the `fasttime` variable. This information is sometimes used during truncation to determine the range bins that can be truncated. Dimension is time.	seconds
`altitude`	WGS 84 geodetic elevation coordinate of the measurement's phase center. Dimension is time.	meters
`amplitude`	Amplitude of low/high gain merged radar reflection after processing.	counts in dB
`fasttime`	Two-way travel time (fast time). Zero time is the time at which the transmit waveform begins to radiate from the transmit antenna.	microseconds
`heading`	Platform heading attitude (zero is north, positive to east). Dimension is time.	degrees
`lat`	WGS 84 geodetic latitude coordinate of the measurement's phase center. Always referenced to north. Dimension is time.	degrees
`lon`	WGS 84 geodetic longitude coordinate of the measurement phase center. Always referenced to east. Dimension is time.	degrees
`pitch`	Platform pitch attitude (zero is level flight, positive is up). Dimension is time.	degrees
`roll`	Platform roll attitude (zero is level flight, positive is right wing tip down). Dimension is time.	degrees
`time`	Time of day (UTC). This is also known as the slow time dimension. The units contain a string describing seconds since YYYY-MM-DD 00:00:00. This pertains to data sets that wrap over a UTC day boundary causing the parameter to be outside the range [0,86400].	seconds

Parameter	Description	Units
param	Multiple variables with a name containing the string "param". Contains radar and processing settings, and processing software version and time stamp information. Fields of structures are not static and may change from one version to the next.	N/A

1.2 File Information

1.2.1 Format

The data files are in netCDF format. The echogram and flight path images are JPEG files. Each data file is paired with an associated XML file, which contains additional metadata. `Echogram.jpg` files contain depth echograms. The echograms are useful for tracking internal layers and shallow ice thicknesses. `Map.jpg` files show campaign flight locations and flight lines.

The y-axis in the JPEG files shows depth relative to a range around the surface. The surface is in the center of the y-axis and the y-axis is set to a fixed range, usually from 0 to 60 or 80 meters for land ice, and 0 to 4 meters for sea ice.

The radar data are divided into segments. A segment is a contiguous data set in which the radar settings do not change. A day is divided into segments if the radar settings were changed, hard drives were switched, or other operational constraints required that the radar recording be turned off and on. The segment ID is YYYYMMDD_SS where YYYY is the four-digit year (e.g., 2011), MM is the two-digit month from 01 to 12, DD is the two-digit day of the month from 01 to 31, and SS is the segment number from 00 to 99. Segments are always sorted in the order in which the data were collected. Generally, SS starts with 01 and increments by 1 for each new segment, but this is not always the case; only the ordering is guaranteed to match the order of data collection.

Each segment is broken into frames, analogous to satellite SAR scenes, to make analyzing the data easier. Most frames are 50 km long, but some may be longer or shorter so the breaks between frames lie at convenient locations. For example, if a grid is flown, the frames are aligned from adjacent lines. Once the frame boundaries are defined, they will not change from one release to the next or one processing method to the next. The frame ID is a concatenation of the segment ID and a frame number: YYYYMMDD_SS_FFF, where FFF is the frame number from 000 to 999. Generally, FFF starts with 000 or 001 and increments by 1 for each new frame, but this is not always the case; only the ordering is guaranteed.

Frames may overlap slightly so data are duplicated where the overlap occurs. GPS time can be used to remove redundant data from the overlapped sections.

1.2.2 Naming Convention

Files are named according to the following convention and described in more detail in Table 2.

```
IRMCR1B_YYYYMMDD_SS_FFF.nc
IRMCR1B_YYYYMMDD_SS_FFF_Echogram.jpg
IRMCR1B_YYYYMMDD_SS_FFF_Echogram_Picks.jpg
IRMCR1B_YYYYMMDD_SS_FFF_Map.jpg
```

Examples:

```
IRMCR1B_20190403_02_001.nc
IRMCR1B_20190403_02_001_Echogram.jpg
IRMCR1B_20190403_02_001_Echogram_Picks.jpg
IRMCR1B_20190403_02_001_Map.jpg
```

Table 2. File Naming Convention

Variable	Description
IRMCR1B	IceBridge MCoRDS L1B Geolocated Radar Echo Strength Profiles data set
YYYY	Four-digit year of survey
MM	Two-digit month of survey
DD	Two-digit day of survey
SS	Segment number (00 to 99)
FFF	Frame number (000 to 999)
Echogram Echogram_Picks Map	The content of the .jpg files is indicated by appending _Echogram, _Echogram_Picks, or _Map to the file name.

1.2.3 File Contents

Example Echogram Picks and Echogram images are shown in Figure 1.

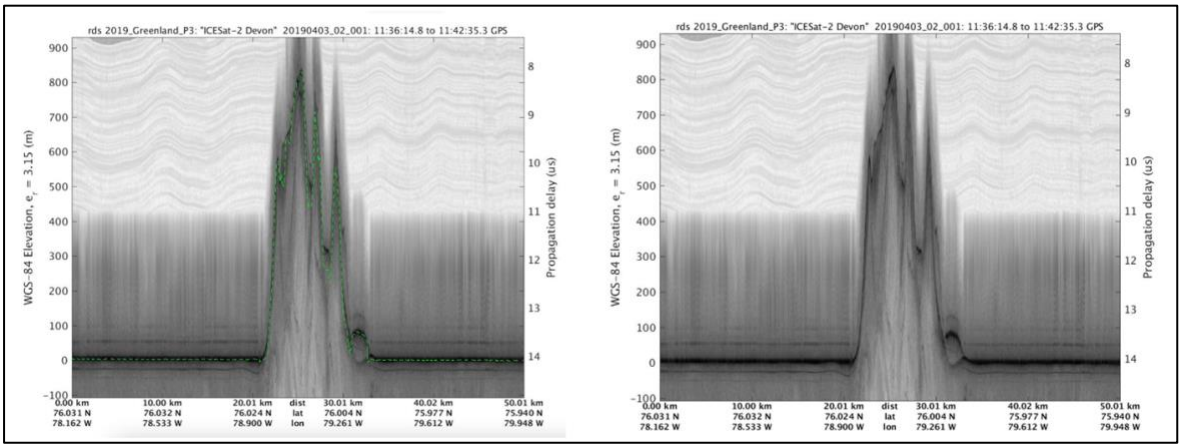

Figure 1. `IRMCR1B_20190403_02_001_Echogram_Picks.jpeg` (left) and `IRMCR1B_20190403_02_001_Echogram.jpeg` (right).

An example Map image is shown in Figure 2.

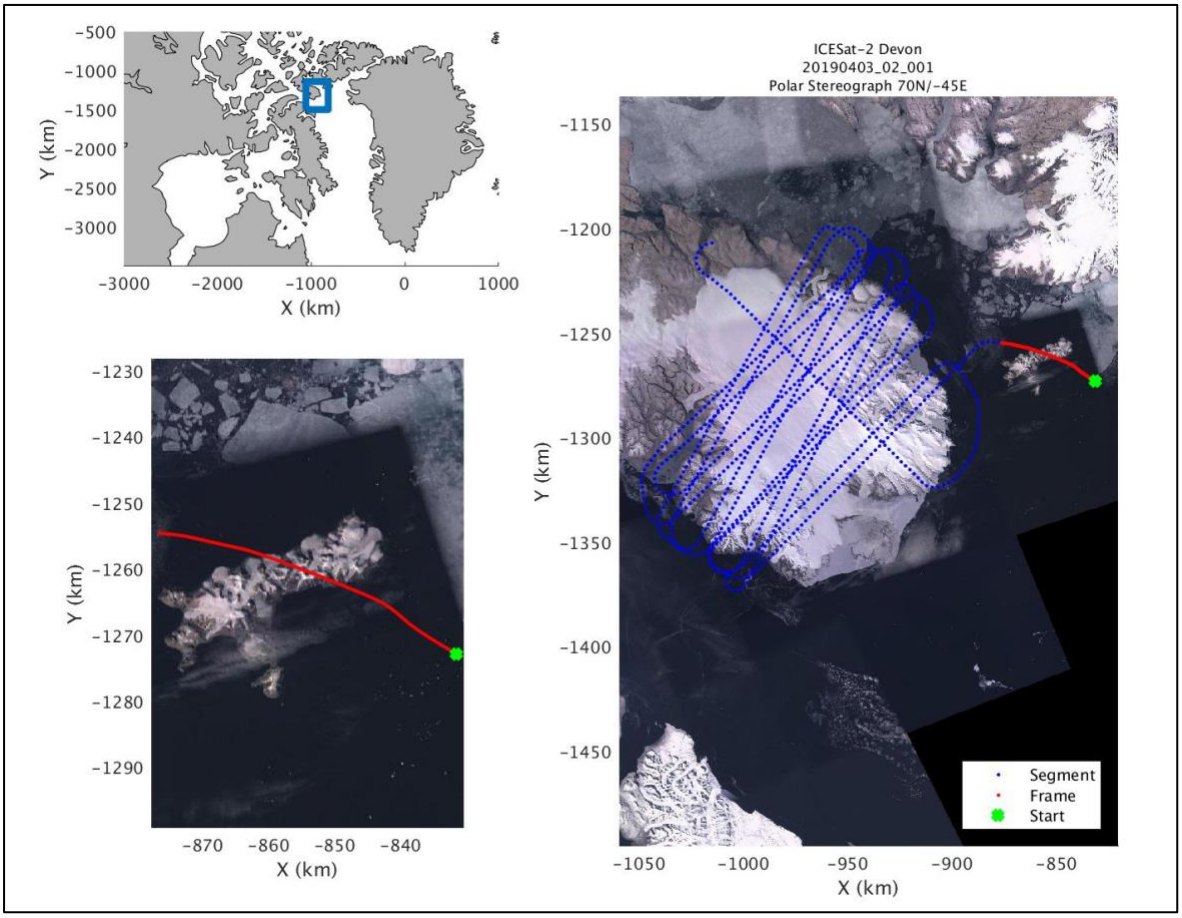

Figure 2. `IRMCR1B_20190403_02_001_Map.jpeg` image.

1.3 Spatial Information

1.3.1 Coverage

Spatial coverage for the IceBridge MCoRDS campaigns includes Antarctica, the Arctic, and Greenland.

Antarctica:
Southernmost Latitude: 90.0° S
Northernmost Latitude: 57.0° S
Westernmost Longitude: 180.0° W
Easternmost Longitude: 180.0° E

Arctic and Greenland:
Southernmost Latitude: 59.0° N
Northernmost Latitude: 83.1° N
Westernmost Longitude: 100.2° W
Easternmost Longitude: 28.5° E

1.3.2 Resolution

Spatial resolution varies dependent on along-track, cross-track, and aircraft height characteristics. See Section 2.5 Processing for further details on resolution and bandwidth.

1.3.3 Geolocation

Table 3. Geolocation Details for the Antarctic Campaigns.

Geographic coordinate system	WGS 84
Projected coordinate system	Antarctic Polar Stereographic
Longitude of origin	0°
Standard parallel	-71°
Datum	WGS 84
Ellipsoid/spheroid	WGS 84
Units	meters
EPSG code	3031
PROJ4 string	+proj=stere +lat_0=-90 +lat_ts=-71 +lon_0=0 +x_0=0 +y_0=0 +datum=WGS84 +units=m +no_defs +type=crs
Reference	https://epsg.io/3031

Table 4. Geolocation Details for the Arctic and Greenland Campaigns.

Geographic coordinate system	WGS 84
Projected coordinate system	NSIDC Sea Ice Polar Stereographic North
Longitude of origin	-45°
Standard parallel	70°
Datum	WGS 84
Ellipsoid/spheroid	WGS 84
Units	meters
EPSG code	3413
PROJ4 string	+proj=stere +lat_0=90 +lat_ts=70 +lon_0=-45 +x_0=0 +y_0=0 +datum=WGS84 +units=m +no_defs +type=crs
Reference	https://epsg.io/3413

1.4 Temporal Information

1.4.1 Coverage

16 October 2009 to 20 November 2019

1.4.2 Resolution

IceBridge campaigns were conducted annually from 2009 to 2019. Arctic and Greenland campaigns were typically conducted in March, April, and May; Antarctic campaigns were typically conducted in October and November.

2 DATA ACQUISITION AND PROCESSING

2.1 Background

For the standard processing output, the receiver-array elements are combined using boxcar or Hanning weights, depending on the frame.

Some of the results are processed through an improved array processing algorithm. The receiver-array elements are combined using the minimum variance distortionless response algorithm which provides improved cross-track clutter rejection. Cross-track clutter rejection is important because the footprint of the antenna array is very large in the cross-track dimension.

2.2 Instrumentation

MCoRDS operates over a 180 to 210 MHz frequency range with multiple receivers developed for airborne sounding and imaging of ice sheets. Measurements are made over two frequency ranges: 189.15 to 198.65 MHz and 180 to 210 MHz. The radar bandwidth is adjustable from 0 to 30 MHz. Multiple receivers permit digital beamsteering for suppressing cross-track surface clutter that can mask weak ice-bed echoes and strip-map SAR images of the ice-bed interface. These radars are flown on twin engine and long-range aircraft including NASA P-3, Twin Otter (TO), and DC-8. GPS time corrections and frames where no reliable sync information was available are given in the records worksheet in the Parameter Spreadsheet.

2.3 Theory of Measurements

When a pulse of radio frequency (RF) energy is transmitted into an ice sheet, a portion of the energy is reflected from the ice surface, ice bottom, and any englacial targets; generally anywhere there is a contrast in the electromagnetic constitutive properties of the media. To detect the ice bottom, lower frequencies are used because they do not attenuate as quickly through ice (Paden, 2005).

Ice thickness is typically determined using data collected from waveforms with different pulse durations. Generally, all receive channels are used to produce the best result. The difference in the propagation time between the ice surface and ice bottom reflections is then converted into ice thickness using an estimated index of refraction of ice (square root of 3.15). The media is assumed to be uniform, that is, no firn correction is applied. See also the related MCoRDS Level 2 data set, *IceBridge MCoRDS L2 Ice Thickness*.

2.3.1 Dynamic Range

The RF signal from the ice surface is typically much larger than that from the ice bottom due to signal attenuation in ice. Generally, different receiver gains are used to capture these signals. Three methods have been used by the radar systems.

Sensitivity Timing Control (STC) is a fast-time gain control where the receiver gain is modified in real-time as the echoes are received. The original sensitivity timing control used a hand dial to control the STC and the STC was analog (not discrete). Radiometric calibration of the data is nearly impossible with these data sets.

Use of low- and high-gain channels results in two separate recordings of the data: one with low receiver gain and one with high receiver gain. This method provides the most flexible and best-

quality dynamic range, but generally doubles the data rate and much of the hardware must be duplicated to capture two channels.

A waveform playlist allows low- and high-gain channels to be multiplexed in time. The low-gain channel typically requires fewer integrations to be useful, so only a small penalty is paid for time multiplexing (3 dB if time was split equally), but typical configurations lose less than 1 dB of sensitivity. Alternatively, two waveforms, one with a short pulse duration and one with a long pulse duration, generally provide better coverage than a single pulse duration. The short pulse duration is used for close-in targets that typically do not require high sensitivity; so, this waveform doubles as the low-gain channel and effectively no penalty is paid for time multiplexing the gain settings. For example, a waveform with a 1 µs duration and lower receiver gain settings is used to measure the round-trip signal time for the ice surface echo, while a waveform with a 10 µs duration and higher receiver gain settings is used to measure the round-trip signal time for the ice bottom echo. As stated above, the two waveforms are used because of the large dynamic range of signal powers that are observed. The 10 µs duration and higher receiver gain settings are more sensitive to the bottom echo, but the signal is generally saturated and unusable from the ice surface and upper internal layers.

For high-altitude data, the difference in power between the ice surface and ice bottom is small enough that a single high-gain setting is possible.

2.4 Acquisition

The signal detection method by aircraft and altitude is described below.

P-3 Low Altitude

A waveform with a 1 µs duration and low receiver gain is used to measure the round-trip signal time for the surface echo, while a waveform with a 10 µs duration and high receiver gain is used to measure the round-trip signal time for the bed echo.

DC-8 Low Altitude

The same concept is used as for P-3. However, during the first two field seasons (2009 Antarctica DC-8 and 2010 Greenland DC-8), extra antennas inside the cabin were used to detect the ice surface delay time because the Transmit/Receive (TR) switches did not meet their switching time specification. In subsequent field seasons, the TR switch control signals were set so that the surface echo was generally still detectable, although with diminished power, even for very low altitudes down to 600 feet Above Ground Level (AGL).

P-3 High Altitude and DC-8 High Altitude

The dynamic range between the ice surface and ice bottom echoes is relatively small and a single high-gain and long-pulse duration waveform is used to capture both echoes.

Twin Otter

Only low-altitude data with waveforms of 1 µs and 10 µs were used, as with P3. A waveform of 20 µs duration was used during some flights to detect the ice bed of the deepest part of the Byrd Glacier trunk.

C-130

Two waveforms of 1 µs and 3 µs duration were used during some flights. Three waveforms of 1 µs, 3 µs, and 10 µs duration were used during other flights. Four waveforms of 1 µs, 3 µs, 10 µs, and 10 µs duration were also used during some flights.

GV

Two waveforms of 1 µs and 3 µs duration were used during low-altitude flights, and two waveforms of 1 µs and 10 µs were used during high-altitude flights.

2.5 Processing

2.5.1 Range Resolution

The range resolution, defined as the minimum range difference to distinguish the return power from two targets with 16 dB of isolation, is determined as:

$$\frac{K_t c}{2B\sqrt{\varepsilon_{r,ice}}}$$

where k_t is the window widening factor (0.88 for no windowing and 1.53 for 20% Tukey time-domain window on transmit and receive and a Hanning frequency-domain window on receive). c is the speed of light in a vacuum; B is bandwidth; and $\varepsilon_{r,ice}$ is the approximate dielectric of ice (3.15). The window widening factor is computed numerically. Windowing is applied to improve the isolation between targets at different ranges but causes the resolution to deteriorate. Table 5 gives the range resolution for several bandwidths.

Table 5. Range Resolution

Bandwidth (MHz)	Range Resolution without Windowing (m)	Range Resolution with Windowing (m)
9.5	7.8	13.6

10	7.4	12.9
17.5	4.2	7.4
20	3.7	6.5
30	2.5	4.3
150	0.5	0.9
180	0.4	0.7

If there is only one target, the range accuracy to that one target is dependent on the signal-to-noise ratio (SNR) given by:

$$\frac{K_t c}{2\mathrm{B}\sqrt{\varepsilon_{\mathrm{r,ice}}}\sqrt{2\cdot\mathrm{SNR}}}$$

Table 6 repeats Table 5 with SNR of 20 dB.

Table 6. Range Resolution - One Target

Bandwidth (MHz)	Range Resolution without windowing (m)	Range Resolution with windowing (m)
9.5	0.55	0.96
10	0.53	0.91
17.5	0.30	0.52
20	0.26	0.46
30	0.18	0.30
150	0.04	0.06
180	0.03	0.05

2.5.2 Along-track Resolution

The along-track resolution depends on the processing method. The default processing parameters starting on 1 March 2012 are described here. For the Single Look Complex (SLC) SAR-processed image (not quick look), a fixed along-track resolution of $\sigma x,SLC$ = 5 m is used. The final product has 11 along-track looks and 1 range look and is then decimated by 6. Therefore, the final product has an along-track resolution of σx = 55 m and a sample spacing of 30 m. The synthetic aperture length, L, is approximately:

$$L \approx \frac{\lambda_c\left(H + T/\sqrt{\varepsilon_{\mathrm{r,ice}}}\right)}{2\sigma_{x,SLC}} K_x$$

where λ_c is the wavelength at the center frequency, *H* is the height above the air/ice interface, *T* is the ice thickness, $\varepsilon_{r,ice}$ is the approximate dielectric of ice (3.15), K_x is the along-track windowing factor for a 20% tukey window (1.1), and $\sigma_{x,SLC}$ is the fixed along-track resolution (5 m).

The Doppler beam width, βx, used in the SAR processing is approximately:

$$\beta_x \approx \frac{\lambda_c}{2\sigma_{x,SLC}} K_x = 9.7 \text{ deg}$$

2.5.3 Cross-track Resolution

While the range and along-track position are known at a fine resolution, the cross-track resolution is poor. For a rough surface, the off-nadir echoes can mask the nadir echo and an off-nadir return may be selected as the ice bottom rather than the nadir return. The best-case scenario is to include crossovers in the data set to estimate the precision of the ice bottom layer picks.

For a smooth surface with no appreciable roughness, the cross-track resolution is constrained to the first Fresnel zone, which is approximately:

$$\sigma_{y,\text{Fresnel}-\text{limited}} = \sqrt{2\left(H + T/\sqrt{\varepsilon_{r,ice}}\right)\lambda_c}$$

where *H* is the height above the air/ice interface, *T* is ice thickness, $\varepsilon_{r,ice}$ is the approximate dielectric of ice (3.15), and λ_c is the wavelength at the center frequency. Table 7 gives the cross-track resolution for several frequencies.

Table 7. Cross-track Resolution

Center Frequency (MHz)	Cross-track Resolution H = 500 m T = 2000 m (m)	Cross-track Resolution H = 8000 m T = 2000 m (m)
125	88.3	209.2
150	80.6	191.0
195	70.7	167.5
210	68.2	161.4

For a rough surface with no appreciable layover, the cross-track resolution is constrained by the pulse-limited footprint, which is approximately:

$$\sigma_{y,\text{pulse}-\text{limited}} = 2\sqrt{\frac{\left(H + T/\sqrt{\varepsilon_{r,ice}}\right)cK_t}{B}}$$

where H is the height above the air/ice interface, T is the ice thickness, $\varepsilon_{r,ice}$ is the approximate dielectric of ice (3.15), c is the speed of light in a vacuum, K_t is the window widening factor, and B is the bandwidth.

Table 8 gives the cross-track resolution with windowing.

Table 8. Cross-track Resolution with Windowing

Bandwidth (MHz)	Cross-track Resolution H = 500 m T = 2000 m (m)	Cross-track Resolution H = 500 m T = 8000 m (m)
9.5	561	1328
10	546	1294
17.5	413	978
20	386	915
30	315	747
150	141	334
180	129	305

For a rough surface where layover occurs, the cross-track resolution is set by the beamwidth β_y of the antenna array. The antenna beamwidth is approximately:

$$\beta_y = \sin^{-1}\frac{\lambda_c}{Nd_y}$$

where B_y is the beamwidth of antenna array, λ_c is the wavelength at the center frequency, N is the number of elements, and d_y is the element spacing. Table 9 gives the beamwidth for the various platforms.

Table 9. Beamwidth for Various Platforms

Platform	N	d_y (λ_c)	Beamwidth (deg)
P-3 original	4	0.5	30.0
TO	4	0.5	30.0
TO	5	0.5	23.6
TO	6	0.5	19.5
P-3 new (center-array only)	7	0.5	16.6
DC-8	5	0.25	53.1
C-130	2	6.35/4.13	98.6/85.8
GV	4	0.47	32.4

In the above table, the values 6.35/4.13 and 98.6/85.8 correspond to frequency bands of 180–230 MHz and 180–450 MHz, respectively; the bandwidths were estimated based on high frequency structure simulation.

2.5.4 Antenna Beamwidth

The antenna beamwidth-limited resolution is:

$$\sigma_{y,\text{beamwidth-limited}} = 2\left(H + \frac{T}{\sqrt{\varepsilon_{r,ice}}}\right)\tan\left(\frac{\beta_y K_y}{2}\right)$$

where H is the height above the air/ice interface, T is the ice thickness, $\varepsilon_{r,ice}$ is the approximate dielectric of ice (3.15), β_y is the beamwidth of antenna array in radians, and K_y is the approximate cross-track windowing factor for a Hanning window applied to a small cross-track antenna array (1.3).

Examples of antenna beamwidth-limited resolution are shown in Table 10.

Table 10. Antenna Beamwidth-limited Resolution

Platform	***N***	***d_y*** **(*λ_c*)**	**Cross-track Resolution H = 500 m T = 2000 m**	**Cross-track Resolution H = 500 m T = 8000 m**
P-3 original	4	0.5	1152	3546
TO	4	0.5	1152	3546
TO	5	0.5	893	2747
TO	6	0.5	732	2252
P-3 new (center-array only)	7	0.5	620	1909
DC-8	5	0.25	2237	6887

2.5.5 Dielectric Error

The dielectric error is expected to be on the order of one percent for typical dry ice (Fujita et al., 2000) and no compensation has been done for a firn layer in SAR processing where the ice is treated as a homogeneous medium with a dielectric of 3.15. The dielectric error using the first term of the Taylor series creates an ice thickness dependent error given by

$$\Delta T = \frac{-T}{2}\varepsilon_{\%\text{error}} = \frac{-T}{200}.$$

For an ice thickness of T = 2000, a one percent dielectric error creates a 10 m thickness error.

2.5.6 System Loop Sensitivity

The system loop sensitivity is the SNR with no channel losses (spreading loss, extinction, and backscattering).

$$SNR = \frac{P_t (N_c G \lambda_c)^2 N_{ave} B T_{pd}}{4\pi k T B F \cdot \mathrm{m}^2}$$

where P_t is the total transmit power including system losses, N_c is the number of channels on transmit and receive used in echogram formation, G is the individual antenna element accounting for the ground plane, λ_c is the wavelength at the center frequency in air, N_{ave} is the approximate number of pulses that may be averaged in SAR processing and presumming, B is bandwidth, T_{pd} is pulse duration, k is Boltzmann's constant ($1.38e^{-23}$ WsK^{-1}), T is the approximated noise temperature before the receiver (290 K), F is the approximate noise figure of the receiver (2), and m^2 is 1 meter squared to cancel out units.

System loop sensitivity values are shown in Table 11.

Table 11. Loop Sensitivity Values

Platform	P_t	N_c	G	N_{ave}	T_{pd} (Âµs)	λ_c(m)	Loop Sensitivity (dB)
MCoRDS DC-8	300	5	1	3200	10	1.54	220
MCoRDS P-3	166	7	4	3200	10	1.54	230
MCoRDS TO (150 MHz)	300	6	4	3200	10	2	233
MCoRDS TO	300	6	4	3200	10	1.54	231

2.5.7 Processing Steps

The following processing steps were performed by the data provider.

1. **Conversion from quantization to voltage at the 50-ohm antenna**.
2. **Removal of DC-bias by subtracting the mean from each record**.
3. **Channel compensation between each of the antenna phase centers**. This includes time delay, amplitude, and phase mismatches. The channel equalization coefficients are found by monitoring the relative returns from each channel from the ocean surface at high altitudes, smooth bed returns, and deep internal layers.
4. **Pulse compression with time and frequency domain windows**. Prior to the 2009 Antarctica DC-8 campaign, the transmitted pulse had a boxcar window. From 2009 Antarctica DC-8 onward, all transmitted pulses typically had a 20 percent Tukey window applied in the time domain. The matched filter applied to the received signal is identical to the transmitted waveform, typically assuming an ideal transmission, with a frequency domain window applied. The frequency domain window is usually a boxcar or Hanning window.
5. **Motion compensation for attitude and trajectory lever arm**.

6. **SAR processing with along-track spatial frequency window using f-k migration**. The dielectric model for f-k migration is always a layered media with variation in the z-axis only.
7. **Channel combination**. Channel combination usually combines channels within a sub-array. Standard SAR processed output applies a normalized array window before summing channels. A minimum variance distortionless response (MVDR) algorithm is used for channel combination, and the spatial correlation matrix is estimated from a neighborhood of pixels surrounding the image pixel being combined. Channel combination also includes multi-looking or spatial incoherent power averaging followed by along-track decimation.
8. **Waveform combination**. Echograms from low- and high-gain channels are combined to form a single image. Generally, combination is done Tpd seconds after the surface return where Tpd is the pulse duration of the transmitted chirp.

2.6 Quality, Errors, and Limitations

The high-altitude data are generally lower quality than the low-altitude data for the following reasons:

1. The cross-track antenna resolution is proportional to the range, creating severe layover problems in mountainous terrain.
2. The sidelobes from the 30-microsecond pulse duration mask out some of the returns that otherwise would have had a high enough SNR.
3. The range to target is greater such that the spherical spreading power loss is greater, leading to a lower SNR.

2.6.1 Error Sources

GPS Time Error

The CReSIS accumulation, snow, MCoRDS, and kuband data acquisition systems have a known issue with radar data synchronization and GPS time. When the radar system is initially turned on, the radar system acquires UTC time from the GPS National Marine Electronics Association (NMEA) string. If this is done too soon after the GPS receiver has been turned on, the NMEA string sometimes returns GPS time rather than UTC time. GPS time is 15 seconds ahead of UTC time during the field season. The corrections for the whole day must include the offset (-15 second correction). GPS corrections have been applied to all of the data using a comparison between the accumulation, snow, and kuband radars which have independent GPS receivers. A comparison to geographic features and between ocean surface radar return and GPS elevation is also made to ensure GPS synchronization. GPS time corrections are given in the records worksheet of the Parameter Spreadsheet.

A time stamp error was discovered in the 2012 Antarctica and 2013 Greenland data. The latest leap second (1 July 2012) was not accounted for in the GPS times for these campaigns. The error

affected Version 2 of the Level 1B CReSIS data sets. The October 2012–2014 MCoRDS data were impacted but have since been corrected and re-published.

Additional Error Sources

The data are not radiometrically calibrated. This means that they are not converted to some absolute standard for reflectivity or backscattering analysis. The MCoRDS science team is working on data processing and hardware modifications to do this.

The primary error sources for ice penetrating radar data are system electronic noise, multiple reflectors also known as multiples, and off-nadir reflections. Each of these error sources can create spurious reflections in the trace data leading to false echo layers in profile data. Multiple reflectors arise when the radar energy reflects off three surfaces back-and-forth in the vertical dimension, and then returns to the receive antenna. They occur in situations when multiple surfaces are present with high impedance, such as the upper surface (air/ground), the base of the ice or an ice–water interface, and the aircraft body which is also a strong reflector. The radar receiver only records time since the radar pulse was emitted, so the radar energy that traveled the additional path length appears later in time, apparently deeper in the ice or even below the ice–bedrock interface. Note that multiples of a strong continuous reflector have a similar shape but all slopes appear magnified, or doubled in the simplest geometric cases, relative to the main reflection.

Off-nadir reflections can result from crevasse surfaces, water, rock outcrops, or metal structures. Antenna beam structure and processing of the MCoRDS system are designed to reduce these off-nadir reflected energy sources.

For standard processing output from Waveform One only, for thin ice, the longer pulse duration of the high-gain waveform may mean that sidelobes from the surface echo mask the bottom return. In these cases, Waveform Two, with a short pulse duration, can provide a better measurement.

3 VERSION HISTORY

Table 12. Version History Summary

Version	Release Date	Description of Changes
V1	January 2011	IRMCR1B data for 2009 through the 2012 Greenland campaign are in binary format, stored separately as IRMCR1B Version 1. For details on the IRMCR1B Version 1 data, see the Version 1 documentation.
V2	November 2014	Beginning with the 2012 Antarctica campaign, all data are provided in netCDF format. Data from all campaigns prior to 2012 Antarctica will be replaced with netCDF data and added to Version 2.

4 RELATED DATA SETS

IceBridge MCoRDS L2 Ice Thickness

IceBridge MCoRDS L3 Gridded Ice Thickness, Surface, and Bottom

IceBridge Accumulation Radar L1B Geolocated Radar Echo Strength Profiles

IceBridge Ku-Band Radar L1B Geolocated Radar Echo Strength Profiles

IceBridge Snow Radar L1B Geolocated Radar Echo Strength Profiles

5 RELATED WEBSITES

CReSIS at KU

IceBridge data at NSIDC

IceBridge website at NASA

ICESat/GLAS at NASA

ICESat/GLAS at NSIDC

6 ACKNOWLEDGEMENTS

The radar systems and software were developed with funding from a variety of sources including NASA (NNX16AH54G), NSF (ACI-1443054), and the State of Kansas. The Operation IceBridge data were collected as part of the NASA Operation IceBridge project. The processing requires GPS and attitude data that are made available by various groups including the Airborne Topographic Mapper team, the Digital Mapping System team, and the Sanders Geophysics company. We also acknowledge all the personnel involved in supporting the field operations.

7 REFERENCES

Akins, T. L. (1999). *Design and development of an improved data acquisition system for the coherent radar depth sounder* [Master's thesis]. University of Kansas.

Allen, C., Shi, L., Hale, R., Leuschen, C., Paden, J., Panzer, B., Arnold, E., Blake, W., Rodriguez-Morales, F., Ledford, J., & Seguin, S. (2012). Antarctic Ice Depth Sounding Radar Instrumentation for the NASA DC-8. *IEEE Aerospace and Electronic Systems Magazine*, *27*(3), 4–20. https://doi.org/10.1109/MAES.2012.6196253

Blake, W., Ledford, J., Allen, C., Leuschen, C., Gogineni, S., Rodriguez-Morales, F., & Shi, L. (2008). A VHF Radar for Deployment on a UAV for Basal Imaging of Polar Ice. *IEEE International Geoscience and Remote Sensing Symposium*, 4: IV-498-IV-501. https://doi.org/10.1109/IGARSS.2008.4779767

Byers, K. J. (2011). *Integration of a 15-Element, VHF Bow-Tie Antenna Array into an Aerodynamic Fairing on a NASA P-3 Aircraft* [Master's thesis]. University of Kansas.

Byers, K. J. (2011). *Integration of a 15-Element, VHF Bow-Tie Antenna Array into an Aerodynamic Fairing on a NASA P-3 Aircraft* [Master's thesis]. University of Kansas.

Chuah, T. S. (1997). Design and Development of a Coherent Radar Depth Sounder for Measurement of Greenland Ice Sheet Thickness. *CReSIS Technical Report*, 151, 175.

Fujita, S., Matsuoka, T., Ishida, T., Matsuoka, K., & Mae, S. (2000). A Summary of the Complex Dielectric Permittivity of Ice in the Megahertz Range and its Application for Radar Sounding of Polar Ice Sheets. *International Symposium on Physics of Ice Core Records. Shikotsukohan, Hokkaido, Japan, September 14–17, 1998*, 185–212.

Gogineni, S., Chuah, T., Allen, C., Jezek, K., & Moore, R. K. (1998). An Improved Coherent Radar Depth Sounder. *Journal of Glaciology, 44*(148): 659–669.

Gogineni, S., Tammana, D., Braaten, D., Leuschen, C., Akins, T., Legarsky, J., Kanagaratnam, P., Stiles, J., Allen, C., & Jezek, K. (2001). Coherent Radar Ice Thickness Measurements Over the Greenland Ice Sheet. *Journal of Geophysical Research-Atmospheres,* 106(D24), 33761–33772.

Lei S., Allen, C. T., Ledford, J. R., Rodriguez-Morales, F., Blake, W. A., Panzer, B. G., Prokopiack, S. C., Leuschen, C. J., & Gogineni, S. (2010). Multichannel Coherent Radar Depth Sounder for NASA Operation Ice Bridge. *IEEE International Geoscience and Remote Sensing Symposium (IGARSS)*, 1729–1732. https://doi.org/10.1109/IGARSS.2010.5649518

Leuschen, C., Allen, C., Gogineni, P., Rodriguez, F., Paden, J., & Li, J. (2011). *IceBridge Snow Radar L1B Geolocated Radar Echo Strength Profiles* [Data set]. Boulder, Colorado USA: National Snow and Ice Data Center.

Leuschen, C., & Allen, C. (2010) *IceBridge MCoRDS L1B Geolocated Radar Echo Strength Profiles* [Data set]. Boulder, Colorado USA: National Snow and Ice Data Center.

Leuschen, C., Allen, C., Gogineni, P., Rodriguez, F., Paden, J., & Li, J. (2011). *IceBridge MCoRDS L3 Gridded Ice Thickness, Surface, and Bottom* [Data set]. Boulder, Colorado USA: National Snow and Ice Data Center.

Li, J., Paden, J., Leuschen, C., Rodriguez-Morales, F., Hale, R., Arnold, E., Crowe, R., Gomez-Garcia, D., & Gogineni, P. (2013). High-Altitude Radar Measurements of Ice Thickness over the Antarctic and Greenland Ice Sheets as a part of Operation Ice Bridge. *IEEE Transactions on Geoscience and Remote Sensing*, *51*(2), 742–754. https://doi.org/10.1109/TGRS.2012.2203822

Namburi, S. P. V. (2003). *Design and Development of an Advanced Coherent Radar Depth Sounder* [Master's thesis]. University of Kansas.

Paden, J., Allen, C., Gogineni, S., Jezek, K., Dahl-Jensen, D., & Larsen, L. (2005). Wideband measurements of ice sheet attenuation and basal scattering. *IEEE Geoscience and Remote Sensing Letters*, *2*(2). https://doi.org/10.1109/LGRS.2004.842474

Paden, J. (2006). *Synthetic Aperture Radar for Imaging the Basal Conditions of the Polar Ice Sheets* [Doctoral dissertation]. University of Kansas.

Paden, J., Akins, T., Dunson, D., Allen, C., & Gogineni, P. (2010). Ice-sheet bed 3-D tomography. *Journal of Glaciology, 56*(195), 3–11. https://doi.org/10.3189/002214310791190811

Player, K., Shi, L., Allen, C., Leuschen, C., Ledford, J., Rodriguez-Morales, F., Blake, W., Panzer, B., & Seguin, S. (2010). A Multi-Channel Depth-Sounding Radar with an Improved Power Amplifier. *High-Frequency Electronics*, 18–29.

Rodriguez-Morales, F., Gogineni, P., Leuschen, C., Allen, C. T., Lewis, C., Patel, A., Shi, L., Blake, W., Panzer, B., Byers, K., Crowe, R., Smith, L., & Gifford, C. (2010). Development of a Multi-Frequency Airborne Radar Instrumentation Package for Ice Sheet Mapping and Imaging. *2010 IEEE MTT-S International Microwave Symposium*, Anaheim, CA, 157–160. https://doi.org/10.1109/MWSYM.2010.5518197

Shi, L., Allen, C. T., Ledford, J. R., Rodriguez-Morales, F., Blake, W. A., Panzer, B. G., Prokopiack, S. C., Leuschen, C. J., & Gogineni, S. (2010). Multichannel Coherent Radar Depth Sounder for NASA Operation Ice Bridge. *IEEE International Geoscience and Remote Sensing Symposium*, 1729–1732. https://doi.org/10.1109/IGARSS.2010.5649518

8 DOCUMENT INFORMATION

8.1 Publication Date

February 2017

8.2 Date Last Updated

January 2023